



Integrating spectral indices into prediction models of soil phosphorus in a subtropical wetland

R.G. Rivero^{a,b,*}, S. Grunwald^{a,b}, M.W. Binford^c, T.Z. Osborne^d

^a GIS Research Laboratory, Soil and Water Science Department, University of Florida, Institute of Food and Agricultural Sciences, 2169 McCarty Hall, P.O. Box 110290, Gainesville, FL 32611, United States

^b School of Natural Resources and Environment, University of Florida, 103 Black Hall, P.O. Box 116455, Gainesville, FL 32611, United States

^c Department of Geography, University of Florida, 3141 Turlington Hall, P.O. Box 117315, Gainesville FL 32611, United States

^d Wetland Biogeochemistry Laboratory, Soil and Water Science Department, Institute of Food and Agricultural Sciences, University of Florida, 106 Newell Hall, P.O. Box 110510, Gainesville, FL 32611, United States

ARTICLE INFO

Article history:

Received 2 September 2008

Received in revised form 2 July 2009

Accepted 2 July 2009

Keywords:

GIS
Remote sensing
Soil
Biogeochemistry
Everglades
WCA-2A
Prediction models
Phosphorus
Wetlands
Ecology
Ecosystem restoration

ABSTRACT

Remote sensing, in combination with multivariate geostatistical methods, has the potential to improve the prediction of soil properties at landscape scales. In the Everglades region, and particularly in Water Conservation Area 2A (WCA-2A), phosphorus enrichment has drawn a lot of attention and has led to an extensive documentation of different aspects of the degradation of the system. This study presents a hybrid geospatial modeling approach to predict soil total phosphorus (TP) using remotely-sensed data and ancillary landscape properties as supporting variables. Two remote sensors, Landsat 7 Enhanced Thematic Mapper (ETM)+ and Advanced Spaceborne Thermal Emission and Reflection Radiometer (ASTER), were used to investigate relationships between spectral data and indices and soil TP. A variation of a vegetation index (Normalized Difference Vegetation Index – NDVI green) was found to be the most effective in predicting floc TP values, due to its capacity to capture small variations in chlorophyll *a* that are associated to TP levels in periphyton, especially in aquatic/non-impacted areas. On the other hand, NDVI, a more traditionally used vegetation index, was still a good indicator of TP variability, particularly in the soil surface layer, due to its stronger relationship with impacted areas dominated by cattail (*Typha domingensis* Pers.). Findings from this study indicate that: a) remote sensing can play an important role in optimizing monitoring of environmental variables, particularly below-ground properties of floc and soils; b) because of limitations about the numbers and frequency of soil samples that can be taken, the combination of remote sensing and geostatistics could represent a non-invasive and cost-effective method to monitor soil nutrient status in complex wetland systems, and c) variations of traditional remote sensing indices such as NDVI can be used to better capture the spatial variability associated with soil and periphyton TP.

© 2009 Elsevier Inc. All rights reserved.

1. Introduction

Wetlands are highly complex ecosystems consisting of mixtures of open water, ridges and sloughs, macrophytes, hammocks/trees, periphyton, flocculent material/detritus, and soils. Some of these ecosystem components can be directly captured (e.g., vegetation, water) or derived with the assistance of remote sensing data. Other properties (e.g., soils) that are not directly sensed can be inferred via statistical relationships combining above-ground and submerged components. Such inferential models that relate remote sensing data to site-specific soil observations in subtropical wetland have been presented by Rivero et al. (2007a) and Grunwald et al. (2007a).

Unlike other aquatic ecosystems, wetlands represent a challenge because they require integrating our knowledge about remote sensing applications for both terrestrial and aquatic ecosystems. There is a need to revise and adapt spectral indices and methods that have been developed for specific aquatic or terrestrial ecosystem components to better capture and understand the diversity and variability of the various communities and features present in wetlands. Larger wetlands such as the Greater Everglades (Noe et al., 2001) and Pantanal (Junka and Nunes de Cunhab, 2005) have been impacted by anthropogenic nutrient influx that altered their structure, functions, and resilience. Characterization of soil nutrient status in these wetland ecosystems is needed to design and implement management systems that reverse ecological degradation.

Multispectral scanners, such as Landsat, Satellite Pour l'Observation de la Terre (SPOT), and Advanced Spaceborne Thermal Emission and Reflection Radiometer (ASTER), have been used in the mapping of wetlands, and wetland change detection analysis with considerable

* Corresponding author. Current address: Everglades Foundation, 18001 Old Cutler Road, Suite 625, Miami FL 33157, United States. Tel.: +1 305 251 0001x232; fax: +1 305 251 0039.

E-mail address: rrivero@evergladesfoundation.org (R.G. Rivero).

accuracy. Ozesmi and Bauer (2002) provided a general review of remote sensing applications in wetlands, while other authors have focused on specific applications in the USA (Ackleson & Klemas, 1987; Sader et al., 1995; Sahagian & Melack, 1996; Baban, 1997; Lo & Watson, 1998; Townsend & Walsh, 2001), South America (Gleiser et al., 1997; Mertes et al., 1993), Africa (Pope et al., 1992; Haack, 1996; Munyati, 2000), and Australia (Johnston & Barson, 1993; Harvey & Hill, 2001). Although the most widely use of remote sensing has been on vegetation classification and land cover mapping, other uses have been monitoring of biomass changes and stress on wetland vegetation. Many studies have evaluated the ability of remote sensing to quantify biophysical measures such as leaf area index (LAI), the fraction of absorbed photosynthetically active radiation (FAPAR) and biomass (Numata et al., 2003). However, not much research has been presented in correlating remotely-sensed spectral responses with biogeochemical properties of soils (Grunwald et al., 2007a).

Wetland soils provide a memory of natural and anthropogenic stresses including fire, hurricanes and tropical storms, point and non-point source pollution and hydrologic change. Soils are a highly variable, dynamic component of the environment and sustainability of soil resources is essential for ecosystem function (Ustin et al., 2004). Thus, understanding the spatial distribution and variability of soil biogeochemical properties, including soil total phosphorus (TP) and their relationship with other ecological properties, is essential for ecosystem assessment, restoration and management.

The objective of this study was to evaluate the use of spectral signatures and indices from two remote sensors (ASTER, and Landsat 7 Enhanced Thematic Mapper, ETM+) to improve predictions of TP in soils using inferential models in a subtropical wetland. We focused on floc, the top layer of unconsolidated organic matter, and the surface soil, composed by the 10 cm of consolidated surface peat. We hypothesize that vegetation and water indices derived from ASTER and Landsat ETM+ are capable of capturing subtle changes in chlorophyll *a* and carotenoids in the terrestrial and aquatic vegetation and will produce the best quantitative functional relationships with floc and soil surface TP. The specific hypotheses were: a) areas with high TP concentrations have increased Normalized Difference Vegetation Index (NDVI), showing as a consequence of higher absorbance by chlorophyll in the visible bands from the dominant cattail (*Typha domingensis* Pers.) vegetation, and b) non-impacted areas with low TP concentrations have low reflectance in the infrared (IR) band and high reflectance in the green band, driven by the chlorophyll *a* and carotenoids content in sawgrass (*Cladium jamaicense* Crantz) and periphyton.

2. Remote sensing spectra and vegetation indices

Remote sensing can be used to measure biophysical vegetation properties (e.g., chlorophyll content) and productivity in both vegetation and in the assemblage of algae and microorganisms (periphyton) that is present in the aquatic portion of the system. Since vegetation and periphyton are sensitive to soil nutrient enrichment inference models have value to estimate the magnitude and distribution of nutrient enrichment in soils across both impacted and non-impacted areas (Rivero et al., 2007b). Indirect, statistical relationships may exist between spectral signatures and below-ground properties (e.g., soil TP at 0–10 or 10–20 cm depth) in wetlands. These empirical models can be used as cheap and cost-effective measurements derived by remote sensing in order to improve predictions from costly, labor-intensive and typically sparsely measured soil properties (Grunwald, 2006).

Griffith (2002) provided an extensive review of a variety of remote sensing imagery that can be used for assessing aquatic ecosystems and water quality. He also evaluated the potential of NDVI and NDVI-derived metrics for watershed monitoring and water quality assessment as well as its sensitivity to biophysical character-

istics of vegetation such as leaf area, net primary productivity, levels of photosynthetic activity, and vegetation phenology. The NDVI and vegetation phenological metrics (VPM) may serve as early-warning signals of stress to aquatic ecosystems (Munn, 1988; Kelly & Harwell, 1990).

A recent study found strong correlations between above-ground properties detectable with remote sensing (e.g., NDVI, water band index) and other ecosystem properties related to soil and water, such as ecosystem microbial respiration (Boelman et al., 2003). Narrow spectral bands can measure many individual absorption features of interest to ecologists, such as pigment composition and content (Gitelson & Merzlyak, 1997), canopy water content (Peñuelas et al., 1997), canopy dry litter or wood (Asner et al., 1998) and other properties of foliar chemistry (Curran, 1989; Martin & Aber, 1997). The use of vegetation indices assists in identifying relationships with some of these properties. These indices also surpass the limitations of single wavebands, minimizing external or environmental factors such as lighting conditions, view and solar angles, and background reflection, and thus tend to correlate better with chlorophyll content (Carter et al., 1996).

The NDVI has been probably the most widely studied of these indices. Developed by Rouse et al. (1973) it has been adopted and applied as a proxy in ecological applications, as reviewed by Boelman et al. (2003). The NDVI uses the characteristic “red edge” feature of plant spectra as an indicator of plant vigor. However, some vegetation indices that combine near-infrared (NIR) and red bands minimize background interference, but are less sensitive to chlorophyll concentration, while others that combine NIR and another visible band are more sensitive to chlorophyll concentration (Daughtry et al., 2000).

The green edge, centered around 520 nm (Horler et al., 1983) has been found to be very similar to that of the red edge that is based on the spectral region at the limit of the red and near-infrared wavelengths (680–780 nm) characterized by a sharp rise in the plant reflectance (Filela & Peñuelas, 1994; Horler et al., 1983). Gitelson and Merzlyak (1997) pointed out that the green edge is primarily determined by a mix of carotenoids, chlorophylls *a* and *b*, while the red edge is primarily driven by chlorophyll *a*. The green band tends to be sensitive to changes in chlorophyll especially in areas with low concentration of nutrients suggesting their potential use in non-impacted areas of the Everglades.

Arst (2003) used Hyperion hyperspectral imagery of the Baltic Sea to observe seasonal differences in spectral reflectance related to seasonal blooms of cyanobacteria. Reflectance peaks occurred in the green and the IR bands, the latter one coinciding with the last stages of cyanobacteria blooms. Pigments in cyanobacteria are correlated with the following wavelengths: phycocyanin (approximately 595 nm excitation wavelength, and 650 nm, measured wavelength), and phycoerythrin (approximately 530 nm excitation wavelength, and 570 nm measured wavelength) (Matt Previte, YSI – Endeco – Sontek regional manager, personal communication – www.ysi.com, www.sontek.com).

Seasonal differences have been documented in the Everglades by Craighead (1971) and Rutchey and Vilchek (1994, 1999). Rutchey and Vilchek (1994) used SPOT imagery to produce a classification map of vegetation (10 classes) in Water Conservation Area-2A (WCA-2A). They pointed out that classification inaccuracies are due to ambiguous spectral characteristics of periphyton mixed into the vegetation matrix. The microfloral colonies tend to rise to the surface in the late summer and frequently form large floating masses of variable density on the water surface and around the stems of wetland macrophytes (Rutchey & Vilchek, 1994). Based on these results and on a personal communication with one of the authors (Rutchey, personal communication, July 2006), the optimal time to conduct remote sensing analysis in Everglades wetlands is early spring.

3. Study area: Water Conservation Area-2A

3.1. General description

Water Conservation Area-2A (43,281 ha) is a subtropical freshwater marsh located within the Greater Everglades, Florida. This naturally oligotrophic system has been impacted by nutrient inputs from the Everglades Agricultural Area (EAA) through a complex system of levees and canals since the beginning of the 20th century (McCormick et al., 2001). Soil and vegetative patterns in WCA-2A are influenced by wet and dry periods, nutrient influx, invasive species, fire, and other stresses. Table 1 provides an overview of vegetation types and coverage within the study area derived from a vegetation/land cover GIS dataset (Florida Fish and Wildlife Conservation Commission, 2003).

Soils in the area are Histosols and encompass the Everglades and Loxahatchee peat formations that make up the ridge and slough system in the Everglades (Davis, 1994; Gleason et al., 1974). Elevation ranges from 2.0 to 3.6 m above mean sea level (Wu et al., 1997) generating slow sheet flow running approximately north–east to south–west. Surface hydrology is controlled by a system of levees and water control structures along the perimeter of WCA-2A. The major surface water inflow points are the pump station and water control structures located in the northern perimeter of the area.

3.2. Impacted vs. non-impacted areas in Water Conservation Area-2A

The biogeochemistry of soils, water and vegetation in the Everglades, and particularly in WCA-2A, has been greatly affected by nutrient influx from the EAA leading into two general levels of impacts, as defined by several authors: impacted, and non-impacted (DeBusk et al., 2001; Newman et al., 1996; Noe et al., 2001).

Major ecological changes induced by P influx have been associated with the expansion of cattail, in WCA-2A particularly in areas close to water control inflows. The typical *C. jamaicense* Crantz communities have converted to *Typha/Cladium* mixes (Jensen et al., 1995). Soil TP and vegetation associated with these levels of disturbance have been documented extensively. Newman et al. (1996) found significantly higher mean soil TP concentrations in nutrient-enriched areas dominated by cattail when compared to non-impacted areas. Historic soil TP threshold values in impacted areas have been reported as 450 mg kg⁻¹ (Grunwald et al., 2004), 500 mg kg⁻¹ (DeBusk et al., 2001), and 650 mg kg⁻¹ (Wu et al., 1997). Typical soil TP concentrations in non-impacted areas of the Everglades range from 200 mg kg⁻¹ to 500 mg kg⁻¹ (Koch & Reddy, 1992; Craft & Richardson, 1998; Orem et al., 2002). The distance of P enriched areas from water control structures and the extension of cattail-dominant areas have been estimated between 5 and 7 km in the northern portion of WCA-2A (Noe et al., 2001). Higher levels of soil TP and a widespread shift in plant communities and ecotypes have been documented by Davis (1991) and (Newman et al., 1996, 1998). Encroachment of homogeneous monotypic cattail stands in the northern section of the Everglades, including WCA-2A, and a loss of ecotopic features (ridges and sloughs) in the southern part are indicators of change.

Table 1

Vegetation/land cover units in WCA-2A with area and percentage, from the Florida Fish and Wildlife Conservation Commission (2003).

Vegetation/land cover	Area (ha)	%
Sawgrass marsh	26,445	61.1
Freshwater marsh and wet prairie	7012	16.2
Cattail marsh	6838	15.8
Shrub swamp	1731	4.0
Open water	1082	2.5
Hardwood swamp	173	0.4
Total WCA-2A	43,281	100.0

Interior non-impacted waters across much of the Everglades are low in P and relatively high in dissolved minerals. These areas are dominated by a periphyton assemblage of microbial mat communities of microorganisms that grow on submerged surfaces, and are formed by complex assemblages of mainly cyanobacteria, diatoms and eukaryotic algae (McCormick & O'Dell, 1996; McCormick et al., 1996). Periphyton plays an important role in removing dissolved inorganic P (DIP) from the water column in wetland and littoral habitats because of their high affinity for P and rapid response to inputs (Scinto & Reddy, 2003). Periphyton mats store large amounts of P and contribute to the maintenance of low TP availability in the marsh (McCormick et al., 1998).

The types of algae comprising periphyton in WCA-2A are driven by nutrient gradients across the system. McCormick et al. (1999) documented replacement of endemic periphyton communities by algal species typical of more eutrophic waters. Periphyton is dominated by green filamentous algae in impacted areas near the canal, containing higher chlorophyll *a* and bacteriochlorophyll levels than the periphyton in non-impacted areas. Periphyton is more calcareous and dominated by diatoms (fucoxanthin) in non-impacted areas. A close relationship between periphyton P and water column P along the marsh gradient has been demonstrated by McCormick et al. (1998).

3.3. Wetland components in Water Conservation Area-2A

Wetland components that were linked to spectral data in this study included a) floc and soils, b) periphyton, c) vegetation (macrophytes and tree islands), and d) open water.

3.3.1. Floc and soils

We distinguished between flocculent detritus or unconsolidated sediment (called floc) and soil (or peat). The floc layer is formed of unconsolidated organic matter that overlies a fibrous peat layer in many areas of the Everglades, and is variously called muck or unconsolidated peat (DeBusk et al., 2001), or the upper loose detrital layer (Gaiser et al., 2005). According to DeBusk et al. (2001) within the minimally impacted sawgrass marsh of WCA-2A, this floc layer is composed of living and dead periphyton material, while in the highly nutrient-enriched cattail areas, near the S-10 inflows, the floc apparently originates from decaying macrophytes as well as algae and bacteria. In contrast, soil is defined as a consolidated surface layer or peat (DeBusk et al., 2001).

The distinction between floc and periphyton has been used in various wetland studies in the Everglades (Gaiser et al., 2005; Noe et al., 2001; DeBusk et al., 2001). Soil is one of the last ecosystem components among others (water, periphyton, and macrophytes) to show changes in P-enrichment and the most difficult component to detect changes due to its high variability (Noe et al., 2001; Grunwald et al., 2005, 2007b). Soils respond slowly to elevated P levels, in contrast to floc and periphyton that assimilate P rapidly and stimulate other significant biotic alterations. This is consistent with findings that soils become enriched after input levels exceed the capacity of the biota to sequester P from the water column or detritus (Qualls & Richardson, 2000; Gaiser et al., 2005). While microbes and algae control the short-term uptake of P in most wetlands, soil and peat accretion determine long-term storage (Noe et al., 2001).

3.3.2. Periphyton

The periphyton community is an assemblage of algae, bacteria, fungi and microfauna that occurs at the soil surface attached to macrophytes, and at the water surface (Noe et al., 2001; Gaiser et al., 2005). The most common Everglades periphyton occurs in association with eastern purple bladderwort (*Utricularia purpurea*), a submerged aquatic macrophyte common in wet prairie and slough habitats. Three forms of periphyton can be distinguished: a) metaphyton, floating mats, which are either free-floating or associated with floating

macrophytes; b) epiphyton, attached to the submerged stems of both living and dead macrophytes; and c) epipelon, benthic periphyton, overlying the peat soil, associated with sediment microbial communities (McCormick et al., 1998; Newman et al., 2004). Metaphyton and epipelon are the dominant forms of periphyton in WCA-2A.

Periphyton mats tend to be highly calcareous in the Everglades, (calcite contributes 30–70% to dry mass in non-nutrient-enriched settings) and contain an assemblage of oligotrophic benthic algae dominated by blue-green algae and diatoms (Gaiser et al., 2005). These calcareous mats have been replaced by non-mat forming algal communities dominated by chlorophytes (Gaiser et al., 2005). Phosphorus (P) enrichment has been attributed as the cause of the loss of calcareous (calcium-precipitating) periphyton mats dominated by blue-green algae and diatoms to periphyton assemblages dominated by filamentous green algae (McCormick & O'Dell, 1996; McCormick and Stevenson, 1998; Newman et al., 2004). Although the periphyton is a category that is typically not considered when mapping vegetation/land cover in wetlands, it is usually associated with the wet prairies/marsh. Fig. 1 shows three images from soil and periphyton in the Everglades: a) a soil sample location in the Everglades, during spring season, that provides an example of submerged and benthic periphyton, b) a soil core that includes a layer of periphyton at the top, in green and whitish color (indicating also the presence of a shallow calcareous mat overlying the core and limiting the light penetration to deeper water depths during the summer season), and c) an extensive periphyton mat, covering part of WCA-3A during the summer season, where these mats are more common and produced the described effect.

3.3.3. Vegetation: macrophytes and shrub/hardwood swamp communities in tree islands

The general distribution of vegetation communities in WCA-2A is as follows: macrophyte communities including *U. purpurea*, *Eleocharis cellulosa*, *Panicum hemitomom* and *Sagittaria lancifolia* dominate the sloughs; sawgrass (*C. jamaicense* Crantz) tends to dominate the ridges; and cattail (*T. domingensis* Pers.) dominates the nutrient-enriched areas near canals and water control structures. Tree islands are another distinctive vegetated feature of the Everglades wetland landscape, dominated by shrubs and hardwood swamp species. Tree islands are areas of slightly higher elevation than the surrounding freshwater marsh where non-wetland plants have been able to colonize. They contrast with the generally low, treeless vegetation (macrophytes) of the surrounding slough and marsh leading to a distinctive and rich ecologic habitat for vegetative and wildlife species. The importance of tree islands in relation with P and other major nutrients (carbon and nitrogen) is based on the fact that about 6 to 10 times higher P concentrations have been found in them (Orem et al., 2002). The geochemical characteristics of these areas are distinctly different from those in the surrounding slough/marsh. According to Orem et al. (2002) tree islands are net local sinks for nutrients and they are to some extent responsible for maintaining low nutrient levels in the remainder of the Everglades.

3.3.4. Open water

Open water, occupies only a small portion (1047 ha – 2.47%) of WCA-2A, based on measurements from the 2003 land cover / vegetation map (Florida Fish and Wildlife Conservation Commission, 2003). The areal coverage of open water is higher in other areas of the Everglades such as the Shark River Slough or the overdrained portion of WCA-3A south.

4. Methods

4.1. Soil data and field data collection

Soil sampling data for WCA-2A were collected in 2003 at 111 sites between 05/17 and 05/30/2003, based on a random stratified sam-

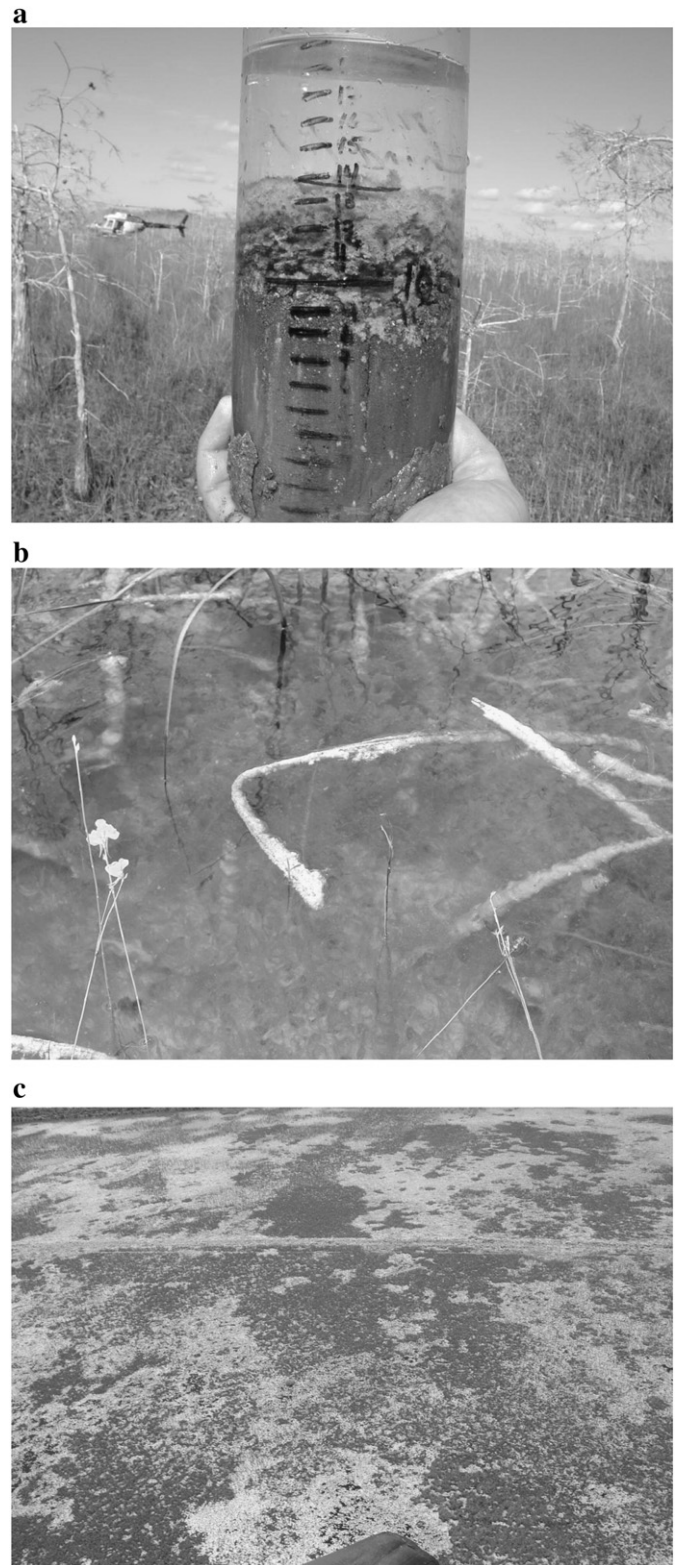


Fig. 1. a). Periphyton in a soil core sample; b). Submerged periphyton overlying floc and soil in the Everglades. c). Overview of floating periphyton mat during wet season (August 2003) in WCA-3A, Everglades (Photos: Todd Osborne, Wetland Biogeochemistry Laboratory, University of Florida).

pling design. Samples were collected and analyzed by the University of Florida Wetland Biogeochemistry Laboratory. Each sampling site was located using a global positioning system (GPS) (Garmin

Table 2
Summary of remote sensing indices algorithms related to vegetation and periphyton.

Index or band ratio	Authors	Algorithms
NDVI	Rouse et al. (1973)	$(R_{860} - R_{660}) / (R_{860} + R_{660})$
NDVI green	Gitelson et al. (1996); Tucker (1979); Daughtry et al. (2000)	$(R_{860} - R_{550}) / (R_{860} + R_{550})$
NDWI	Gao (1996)	$(R_{860} - R_{1240}) / (R_{860} + R_{1240})$
WI	Peñuelas et al. (1993)	(R_{900} / R_{970})

List of acronyms:

NDVI: Normalized Difference Vegetation Index.

NDWI: Normalized Difference Water Index.

WI: Water Index.

NIR: Near-infrared band.

SWIR: Short-wave infrared band.

R refers to reflectance centered at a specific wavelength, shown in subscripts.

International, Inc., Olathe, KS, USA) mounted to a helicopter and labeled with their respective X and Y coordinates in Albers Equal Area Conic map projection. The GPS system was equipped with a real-time Wide Area Augmentation System to ensure a positional accuracy of <3 m to locate the sites. Total phosphorus was determined using an ignition method (Anderson, 1976) followed by the determination of dissolved reactive phosphorus by an automated colorimetric procedure (U.S. Environmental Protection Agency, 1993, Method 365.1). Details of the sampling design, field protocol and laboratory analysis can be found in Rivero et al. (2007b).

4.2. Remote sensing imagery

Two satellite images were selected for the study. The dates of these images are representative of the wet and the dry season: Landsat ETM+, (February 2003, end of dry season) and ASTER (September 2003, end of wet season).

Soil samples were collected in WCA-2A during May 2003, which was constrained by accessibility (water depth) and climatic conditions. We aimed to select satellite imagery as close to the soil sampling campaign as possible. However, the selection of the satellite imagery was limited by the following: (i) images needed to be cloud-free (difficult to achieve during Florida's wet season) to avoid complications with derivation of spectral indices; and (ii) images needed to delineate and distinguish the properties (such as chlorophyll content, periphyton) that were needed to build inferential models with floc/soil TP; thus, climatic/hydrologic and phenological considerations were considered as well.

4.2.1. Landsat 7 Enhanced Thematic Mapper (ETM) +

A Landsat 7 ETM+ scene (path: 15/ row: 42, date 02/13/03), was used for this study. Landsat ETM+ covers an area of 185 × 185 km, and includes seven multispectral bands with 30 m spatial resolution for all bands except band 6, which is a thermal infrared (TIR) band with 60 m spatial resolution, and an additional 15 m panchromatic band. A list of the visible bands is presented in Table 3. This image was obtained and pre-processed by the Florida Fish and Wildlife Conservation Commission (2003).

4.2.2. Advanced Spaceborne Thermal Emission and Reflection Radiometer (ASTER)

An ASTER image from 01/09/2002 was obtained from the US Geological Survey (USGS) – Land Process Distributed Active Archive Center, established as part of the National Aeronautics and Space Administration (NASA) Earth Observing System (EOS) Data and Information System (DIS). The ASTER L1B product (registered radiance at the sensor) contains radiometrically calibrated and geometrically co-registered data for all the channels acquired previously through the telemetry streams of the 3 different telescopes in Level-1A. (Technical Description for ASTER data from: <http://lpdaac.usgs.gov>).

The ASTER sensor covers an area of 60 × 60 km and wide spectral region with 14 bands from visible to thermal infrared. For the analysis the 3 visible and near-infrared radiometer (VNIR) bands with a spatial resolution of 15 m, and the 6 short-wave infrared radiometer (SWIR) bands with a spatial resolution of 30 m were used. The spectral resolution of these images is shown in Table 3.

4.3. Image data processing

The ASTER data was downloaded in HDF-EOS (Hierarchical Data Format) that is the standard data format for all NASA Earth products. The image was imported into ERDAS Imagine Version 9.0 (Leica

Table 3
Summary of 32 parameters evaluated for the prediction model for floc and surface soil TP.

Category	Parameter	Description	Spectral range or algorithm	Source
ASTER Spectral bands	AST B1	ASTER Band 1 (green)	0.52–0.60 mm	
	AST B2	ASTER Band 2 (red)	0.63–0.69 mm	
	AST B3	ASTER Band 3 (NIR) ^a	0.78–0.86 mm	
	AST B4	ASTER Band 4 (SWIR) ^b	1.60 – 1.70 mm	
	AST B5	ASTER Band 5 (SWIR) ^b	2.145–2.185 mm	
	AST B6	ASTER Band 6 (SWIR) ^b	2.185–2.225 mm	
	AST B7	ASTER Band 7 (SWIR) ^b	2.235–2.285 mm	
	AST B8	ASTER Band 8 (SWIR) ^b	2.295–2.365 mm	
	AST B9	ASTER Band 9 (SWIR) ^b	2.350–2.430 mm	
ASTER	AST NDVI	ASTER NDVI ^c	(Bnd 3 – Bnd 2) / (Bnd 3 + Bnd 2)	Rouse et al. (1973)
Indices and PCA	AST NDVI g	ASTER NDVI green	(Bnd 3 – Bnd 1) / (Bnd 3 + Bnd 1)	Tucker (1979)
	AST NDWI	ASTER NDWI ^d	(Bnd 3 – Bnd 4) / (Bnd 3 + Bnd 4)	Gao (1996)
Landsat ETM + Spectral bands	AST PCA1	ASTER PCA1 ^e		
	AST PCA2	ASTER PCA2 ^e		
	AST PCA3	ASTER PCA3 ^e		
	ETM B1	Landsat ETM+ Band 1 (blue)	0.45–0.51 mm	
	ETM B2	Landsat ETM+ Band 2 (green)	0.52–0.60 mm	
	ETM B3	Landsat ETM+ Band 3 (red)	0.63–0.69 mm	
	ETM B4	Landsat ETM+ Band 4 (NIR)	0.75–0.90 mm	
Landsat ETM + Indices and PCA	ETM B5	Landsat ETM+ Band 5 (SWIR)	1.55–1.75 mm	
	ETM B6	Landsat ETM+ Band 7 (SWIR)	2.09–2.35 mm	
	ETM NDVI	Landsat ETM+ NDVI ^c	(Bnd 4 – Bnd 3) / (Bnd 4 + Bnd 3)	Rouse et al. (1973)
	ETM NDVI g	Landsat ETM+ NDVI green	(Bnd 4 – Bnd 2) / (Bnd 4 + Bnd 2)	Tucker (1979)
	ETM NDWI	Landsat ETM+ NDWI ^d	(Bnd 4 – Bnd 5) / (Bnd 4 + Bnd 5)	Gao (1996)
	ETM PCA1	Landsat ETM+ PCA1 ^e		
	ETM PCA2	Landsat ETM+ PCA2 ^e		
	ETM PCA3	Landsat ETM+ PCA3 ^e		
	X UTM	Xcoordinate (UTM)		
	Y UTM	Y coordinate (UTM)		
Dist TI	Distance to tree islands	Tree islands extracted from FWC		FWC ^f
DistWCS	Distance to water control structures			SFWMD ^g
FWC hab	Vegetation/land cover			FWC ++

Each parameter includes category, parameter name, description and spectral range, algorithm and source (when applicable) for WCA-2A.

^a NIR: Near-infrared.

^b SWIR: Short-wave infrared.

^c NDVI: Normalized difference vegetation index.

^d NDWI: Normalized difference water index.

^e PCA: Principal component analysis.

^f FWC: Florida Fish and Wildlife Conservation Commission.

^g SFWMD: South Florida Water Management District.

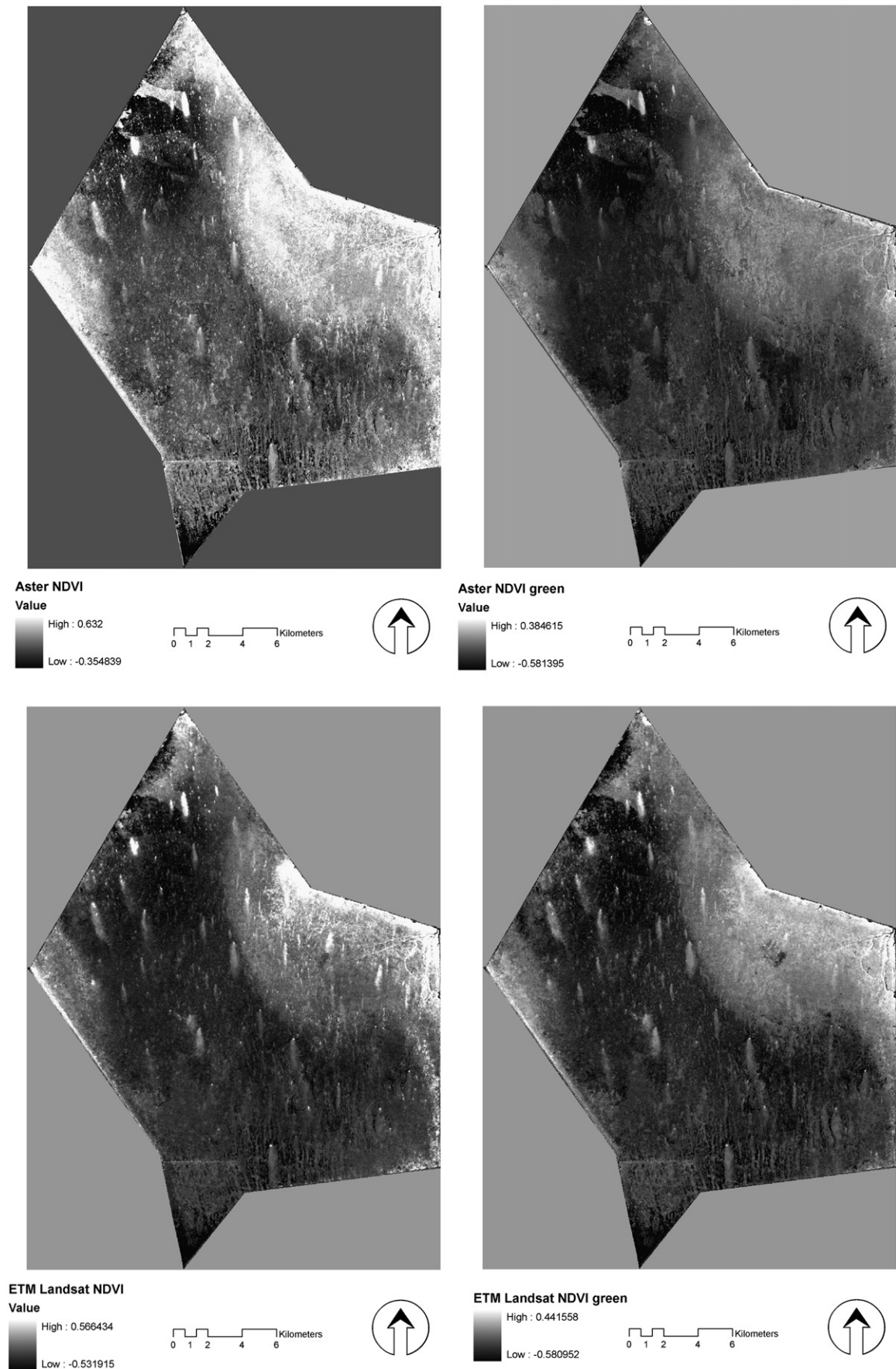


Fig. 2. NDVI and NDVI green maps from ASTER (01/09/2002) and Landsat ETM + (02/13/03) remote sensing data. Highest values are shown in lighter colors and lowest values in darker colors.

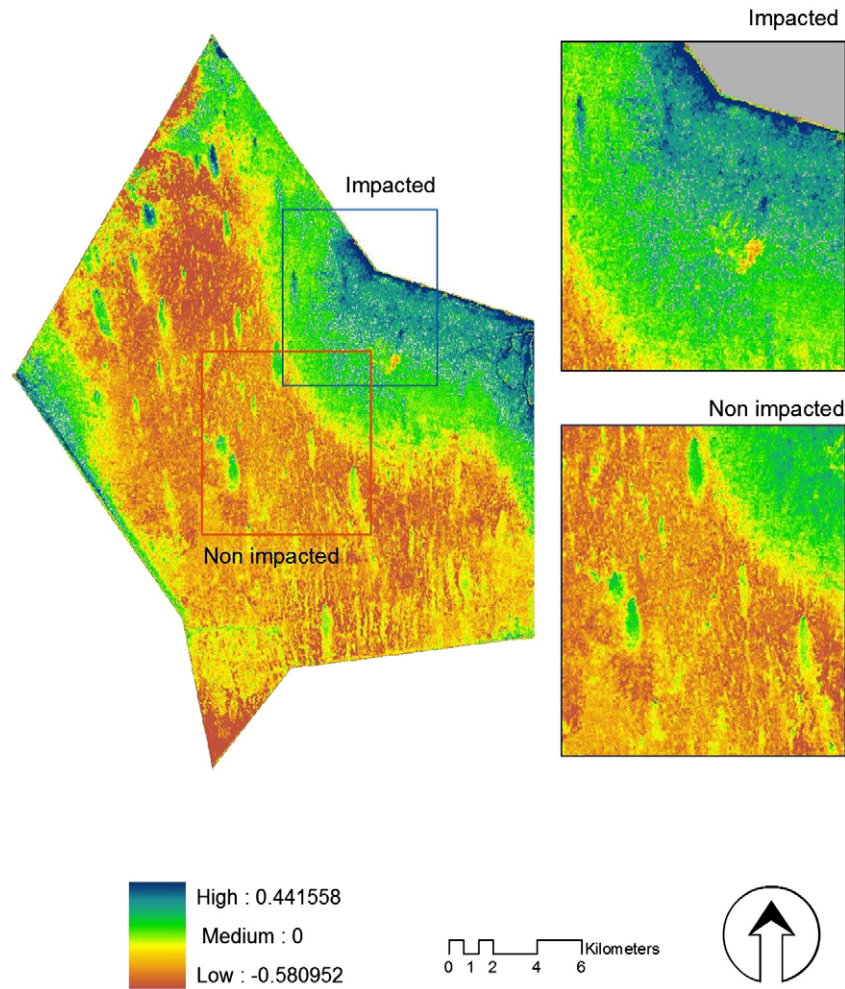


Fig. 3. Landsat ETM+ NDVI green showing a detail of impacted (3a) and non-impacted areas (3b) of WCA-2A.

Geosystems, Atlanta, USA), which allowed conversion from HDF format files. In order to use the first 9 bands for the initial exploration of the bands spectra, the first 3 VNIR bands and the 6 SWIR bands were stacked and SWIR bands (30 m resolution) resampled into the 15 m resolution of the VNIR bands. The ASTER image was geometrically rectified, using USGS digital orthophoto quadrangles (DOQQ) with a total of 35 ground control points that were selected from both the image and the DOQQs. The root mean square error (RMSE) was 0.5 pixel (7.5 m). The Landsat ETM+ image was rectified by FFWCC. Both images were reprojected to a Universal Transverse Mercator (UTM) projection (Zone 17; Datum: NAD 83).

The following spectral indices were derived from Landsat ETM+ and ASTER images: (i) NDVI, (ii) Green Normalized Difference Vegetation Index (NDVI green), and (iii) Normalized Difference Water Index (NDWI). A summary of formula to derive indices is given in Table 2.

Brightness values and spectral indices from Landsat ETM+ and ASTER imagery, respectively, were extracted for each sampling point with the Spatial Analyst extension using ArcGIS 9.1 (Environmental Systems Research Institute – ESRI, Redlands, CA). A principal component analysis (PCA) was performed with both, the 9 stacked ASTER bands and the 6 Landsat ETM+ bands, and the first 3 components for each sensor were incorporated into the analysis.

4.4. Digital ancillary spatial data

Additional ancillary data included a vegetation/land cover map from FFWCC (2003) and USGS DOQQ that were used for geometric

correction and also for visual comparison of vegetation units. A GIS layer of water control structures (South Florida Water Management District, 2005) was used to document the nutrient influx points into WCA-2A. A tree island layer was produced by reclassification of the vegetation/land cover raster dataset from FFWCC.

The Euclidean distance for each pixel in the study area to tree islands and water control structures was calculated using ArcGIS 9.1 Spatial Analyst (ESRI, Redlands, CA) using the Distance/Straight line function. The ArcGIS software was also used to integrate, analyze and display data from different sources and software outputs.

4.5. GIS and statistical analysis

A matrix with 32 parameters, compiled for each of the 111 sampling points, was derived using: a) the remote sensing from ASTER visible and infrared bands (bands 1 to 9), Landsat ETM+ 7 visible and infrared bands (bands 1 to 6) and indices extracted from these, and b) the values extracted from the GIS layers, including vegetation/land cover, distance to canals, distance to tree islands, and X and Y coordinates. Values for each raster were extracted using the Values to Points function in ArcGIS 9.1 (Environmental Systems Research Institute, Redlands, CA). A brief description of each of these parameters is presented in Table 3.

To normalize positively skewed soil sampling data a log transformation was used. The correlation and statistical analysis was conducted with the SPSS statistical package (SPSS v. 14.0 Lead Technologies). Scatterplots were generated for graphical interpretation relating

spectral data and indices to TP in floc and topsoil using land cover/vegetation data as complimentary strata.

We used (i) stepwise linear multivariate regression (SLMR), (ii) non-linear regression (NLR), and (iii) multiple regression to model the relationship between floc and surface soil TP, respectively, and the selected variables showing the highest correlations. The independent variables included spectral data from Landsat ETM+ and ASTER, spectral indices, and ancillary geospatial landscape properties; these were related to dependent variables of TP floc and soil, respectively. The Pearson correlation coefficient (r), coefficient of determination (R^2) and adjusted R^2 were used to evaluate different models.

5. Results

5.1. Maps of remote sensing indices for ASTER and Landsat 7 ETM+ imagery

The NDVI and NDVI green maps for the ASTER and Landsat ETM+ imagery are shown in Fig. 2. The maps show a gradation from black to white, where lighter colors correspond to the higher NDVI and NDVI green values (above 0), and the darker colors correspond to the lowest (close and under 0) NDVI and NDVI green values, respectively. Although the four maps look very similar at first sight, it is evident that the Landsat ETM+ images provided more pronounced differentiation of distinct landscape features such as tree island heads and tails. These are the smallest features with the lightest gray color in the map, located in the central and western portion of the area. They are followed by a light gray color representing areas near canals that are dominated by cattail and cattail/sawgrass mix. The darker areas in the west and central portion correspond to the un-impacted areas dominated by sawgrass and slough communities, with a very small proportion of open water areas. The white and light gray colors are indicative of higher NDVI green values (above 0), associated with impacted areas dominated by cattail, and also with other dense vegetated areas such as tree islands. The NDVI index has a similar response to that of NDVI, with higher reflectance in the NIR band and higher absorbance in the green band. This is due to the chlorophyll *a* content and its implications in the absorbance/reflectance with NDVI green reaching its highest values. Such high NDVI green values are found in areas of dense vegetation dominated by tree island heads and tails (white, values as high as 0.44 in the NDVI green map), and also dense stands of cattail, near canal inflows (white to light gray), where higher TP values were found.

Areas in darker gray, located in the center and west of the area coincide with sawgrass with NDVI green values near 0. Those dark gray to black areas indicate sloughs, with submerged and floating periphyton and very limited extensions of open water. NDVI green values are lower than 0 because of the high reflectance in the green band as a consequence of the chlorophyll *a* and carotenoids content in the periphyton, and the high absorbance in the IR caused by the overlying periphyton. Both NDVI green and soil TP reach their lower values in these un-impacted areas.

Fig. 3 shows details of a Landsat ETM+ NDVI green image, with a gradation from dark blues for most impacted areas to green, in transition and intermediate areas (including tree islands) and from there to browns to non-impacted areas. The mean TP values were 1108 mg kg⁻¹ (floc) and 667 mg kg⁻¹ (surface soil) for areas classified as cattail marsh and 1007 mg kg⁻¹ (floc) and 688 mg kg⁻¹ (surface soil) for areas classified as hardwood swamp corresponding to tree islands (Rivero et al., 2007b). These elevated TP areas showed also the highest mean NDVI green values.

Correlations between floc and soil TP, spectral data and indices, PCA scores and ancillary environmental variables are shown in Table 4. The strongest correlation between floc and soil TP was found with NDVI and NDVI green for both Landsat ETM+ and ASTER remote

sensing data. In general, the correlation coefficients were higher for floc TP than for surface soil TP. These results were expected since floc is the closest layer to the surface and may show stronger relationships to above-ground features when compared to deeper soil layers. The highest correlation coefficient with floc TP, significant at the 0.01 confidence level, was for Landsat ETM+, both NDVI green (0.82) and NDVI (0.73). Conversely, ASTER showed the same correlation coefficient (0.68) between floc TP and NDVI and NDVI green, respectively. For surface soil TP, correlations were not only lower than for floc, but also different, being higher in both cases for NDVI than for NDVI green. The highest correlation values between soil surface TP and Landsat ETM+ were obtained for both NDVI and NDVI green (0.68), while correlations with ASTER were very similar, with NDVI (0.63) and NDVI green (0.62).

Differences in correlations between images and indices were more pronounced for floc TP, than for surface soil TP suggesting a higher variability in TP concentrations within the floc. This is supported by the large range in floc TP with 1671 mg kg⁻¹ when compared to soil TP with 1546 mg kg⁻¹. Standard deviations for floc TP (381 mg kg⁻¹) and soil TP (316 mg kg⁻¹) were comparable.

Negative correlations between the distance to water control structures of -0.74 with floc TP and -0.60 with soil surface TP, respectively, were found indicating the presence of a P-enrichment gradient in WCA-2A that has been documented by numerous authors (Newman et al., 1998; Reddy et al., 1998; DeBusk et al., 2001). This distance gradient extends of about 7 km from the water inflows into the marsh interior. The *y* coordinate showed significant correlations of 0.46 with floc TP and 0.40 with soil surface TP. This may be a response to hydrological flow patterns in the north-south direction, also associated with slight variations in elevation.

Table 4

Pearson correlation coefficients (r) between floc and surface soil total phosphorus (TP) in mg kg⁻¹ and other variables in WCA-2A, Everglades.

Variable	Log floc TP	Log surface soil TP
X UTM	0.196(*)	0.194(*)
Y UTM	0.449(**)	0.397(**)
X ALBERS	0.183	0.182
Y ALBERS	0.455(**)	0.404(**)
ETM NDVI green	0.822(**)	0.678(**)
ETM NDVI	0.725(**)	0.679(**)
AST NDVI	0.681(**)	0.625(**)
AST NDVI green	-0.681(**)	-0.622(**)
Distance to tree islands	0.451(**)	0.347(**)
Distance to control structures	-0.736(**)	-0.603(**)
ETM B1	-0.470(**)	-0.258(**)
ETM B2	-0.343(**)	-0.151
ETM B3	-0.315(**)	-0.251(**)
ETM B4	0.580(**)	0.575(**)
ETM B5	0.484(**)	0.280(**)
ETM B6	0.281(**)	0.095
AST B1	-0.093	0.014
AST B2	0.003	0.026
AST B3	0.487(**)	0.507(**)
AST B4	0.504(**)	0.350(**)
AST B5	0.394(**)	0.267(**)
AST B6	0.374(**)	0.227(*)
AST B7	0.316(**)	0.218(*)
AST B8	0.254(**)	0.124
AST B9	0.256(**)	0.099
AST PCA1	0.365(**)	0.299(**)
AST PCA2	0.487(**)	0.290(**)
AST PCA3	0.524(**)	0.538(**)
ETM PCA1	0.277(**)	0.199(*)
ETM PCA2	-0.505(**)	-0.277(**)
ETM PCA3	0.565(**)	0.587(**)

* Correlation is significant at the 0.05 level (2-tailed).

** Correlation is significant at the 0.01 level (2-tailed).

Our aim was to identify quantitative relationships between floc and soil TP, spectral data and derivatives, and ancillary environmental data. Rather than trying to perform a classification, the scatterplots served as an exploratory tool. Fig. 4 shows scatterplots of Landsat ETM+ and ASTER brightness values extracted for each sampling location. Spectral values of red vs. NIR and green vs. NIR were symbolized with the vegetation/land cover classes. The scatterplots that included the green band (band 1 for ASTER and band 2 for Landsat ETM+) were more concentrated or less dispersed along the center line, than the ones including the red band (band 2 for ASTER and 3 for Landsat ETM+). Scatterplots of different band combinations have been used in the past to graph the location of particular land cover units in feature space. For example, a plot of red versus NIR feature space of measurement vectors for a variety of land cover types within WCA-2A was shown by Jensen et al. (1995), based on historical remote sensed data (MSS 1973, 1976, 1982, and SPOT 1987, 1991). Six vegetation/land cover classes were described by Jensen et al. (1995) based on the location of each unit in feature space, relating them to the red and NIR feature space plot. Cattail reflected more NIR radiant flux while absorbing similar amounts of red radiant flux than the other vegetation and land cover types (sawgrass and cattail/sawgrass mixture). The lowest values, located near the origin in the plot (approximately 30 NIR, 30 red), corresponded to the slough/water type, in response to the higher absorbance of this land cover in both bands. Dense brushes, corresponding to tree island heads and tails, absorbed higher amounts of red radiant flux and reflected more NIR radiant flux than the previous communities.

Similar to Jensen et al. (1995), our results show an overlapping spectral response of some land cover/vegetation units, especially those in the aquatic portion (sawgrass/slough/water). This result was expected since it has been documented that limitations exist to accurately map vegetation in wetland areas (Rutchev and Vilchek, 1994).

A different set of scatterplots was graphed to evaluate relationships of floc TP and surface soil TP with four vegetation indices that showed high correlations: ASTER NDVI and NDVI green and Landsat ETM+ NDVI and NDVI green (Figs. 5 and 6). These plots suggest that relationships exist between floc/soil data and spectral indices. There is a clear trend with the floc NDVI green data that is consistent with the 0.82 correlation coefficient.

The highest R^2 values were obtained by using the NDVI and NDVI green as independent variables to predict the dependent variables floc TP and soil TP, respectively. Results indicated that Landsat ETM+ derived indices had slightly better R^2 when compared to ASTER derived indices to predict floc and soil TP. The R^2 ranged between 0.68 and 0.51 to predict log floc TP and between 0.45 and 0.38 to predict soil TP (Table 5).

A summary of the linear, quadratic and multiple regression equations for both soil layers (floc and soil surface) is presented in Tables 6 and 7, and results from the linear (stepwise) regression analysis and non-linear (quadratic) model are shown in Fig. 7. The results indicate that Landsat ETM+ performed better than ASTER in predicting floc and soil TP concentrations. Although Landsat ETM+ has lower spatial resolution (30 m) than ASTER (15 m) the former was able to better

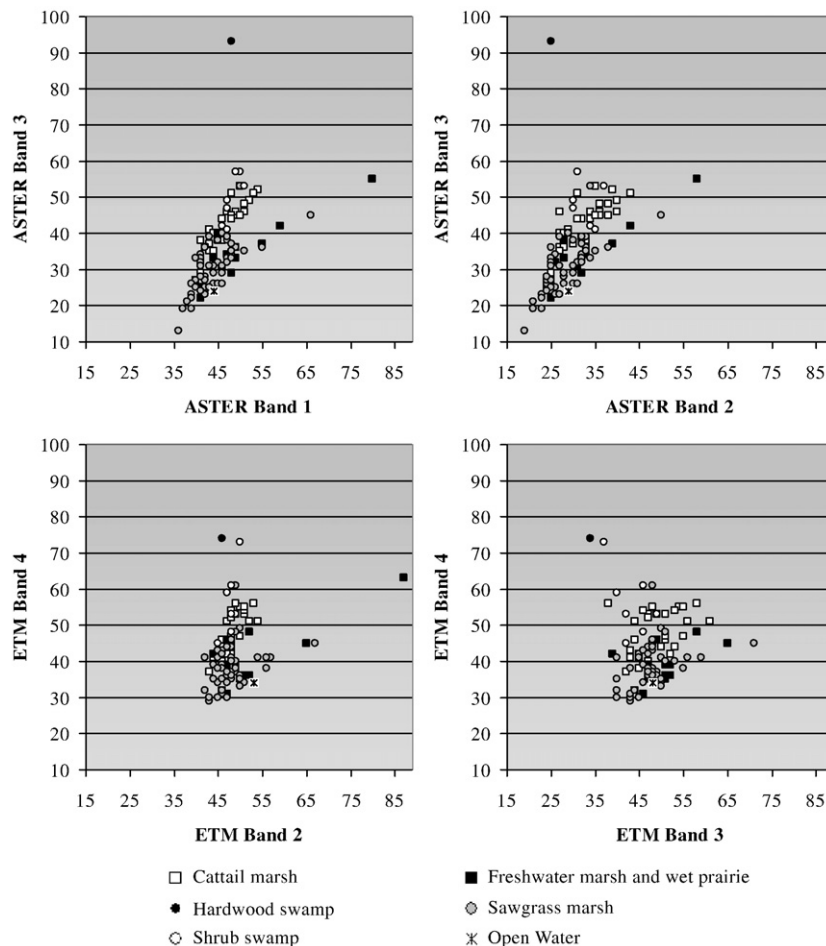


Fig. 4. Scatter plots of ASTER band 1 (green) and band 3 (NIR) – top left; band 2 (red) and band 3 (NIR) – top right, Landsat ETM+ band 2 (green) and band 4 (NIR) – bottom left, and band 3 (red) and band 4 (NIR) – bottom right; symbolized with FWC vegetation/land cover class extracted for each sampling point in WCA-2A.

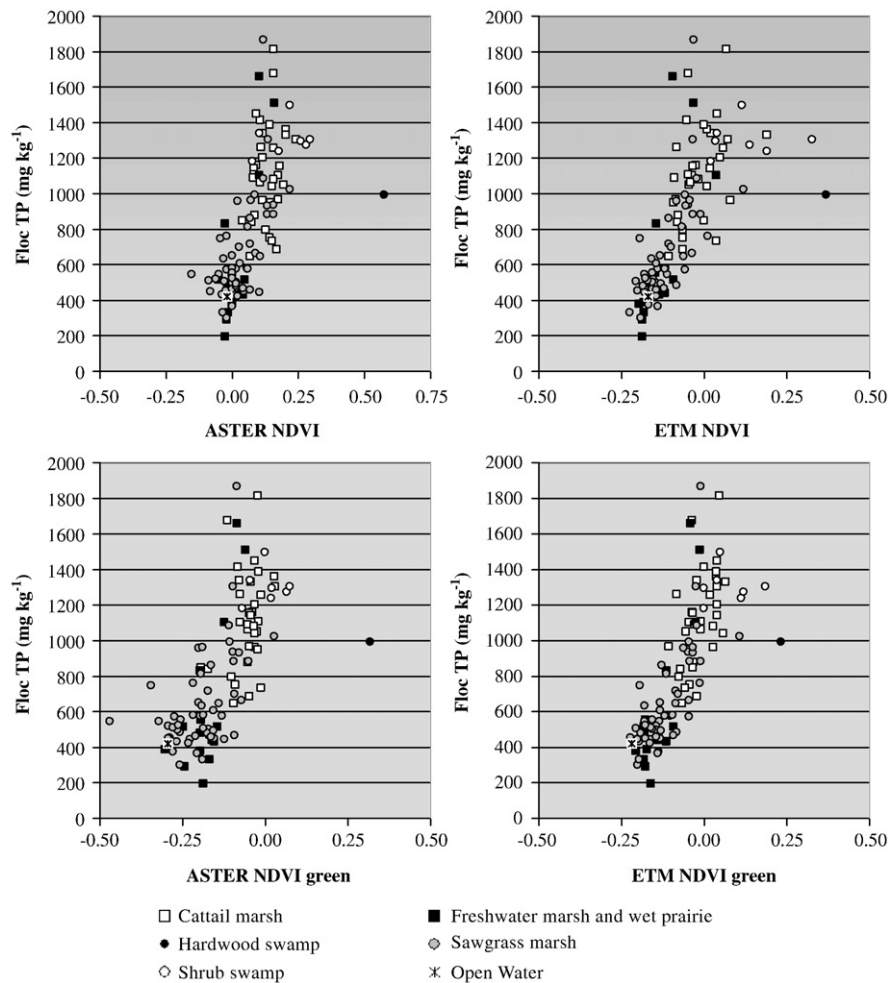


Fig. 5. Scatter plots of floc TP data against ASTER and Landsat ETM+ values for NDVI and NDVI green with symbol indicating FWC vegetation/land cover class extracted for each sampling point in WCA-2A.

capture some of the nutrient heterogeneity in soils, including tree island and ridge/slough dynamics, and soil TP gradients across WCA-2A.

6. Discussion

Our findings suggest that remote sensing indices are capable of capturing subtle changes in the mix of chlorophyll *a* and carotenoids in vegetation and the aquatic portion of WCA-2A, and perform the best in quantifying relationships with floc and soil surface TP. Landsat ETM+ NDVI green was the best predictor for floc TP, and Landsat ETM+ NDVI was the best predictor for soil surface TP in WCA-2A. Our results are consistent with those by Gaiser et al. (2005) showing strong relationships in TP concentrations between floc and periphyton and moderately strong at the soil surface level. This can be explained by P-enrichment trends that are relatively fast in floc but slower in soils. Phosphorus enrichment modifies the structure and function of the Everglades ecosystem due to increases in the concentration of P in most components (water, periphyton, soil, and macrophytes). It also alters biogeochemical processes, eliminates calcareous periphyton mats, deoxygenates soils, accelerates rates of soil accretion and nutrient storage, and stimulates major shifts in plant and animal species composition (Noe et al., 2001; Gaiser et al., 2005; Rutchey and Vilchek, 1994; Reddy et al. 1998).

Soils become enriched after P inputs exceed the capacity of the biota to sequester available P from water column or detritus. The strong relationship between TP content and macrophytes, and par-

ticularly with cattail may elude why NDVI acts as a good predictor for surface soil TP. This interpretation can be supported by the high correlations and strong functional relationships between these two variables. In contrast, the variability of the aquatic component was better captured by the NDVI green index and showed stronger association to periphyton/floc TP.

Quental (2001) investigated remote sensing detection of stress in plants caused by deficit in nutrients. He also pointed out that physiological effects of stress are due to a decrease in leaf chlorophyll concentration and increase of the carotenoids to chlorophyll ratio. In the case of WCA-2A, this would be characteristic of non-impacted areas located far from the canals that have been historically P-limited, dominated by sawgrass and periphyton. In contrast, impacted areas, in proximity of canals that serve as entry points of nutrients into WCA-2A, are composed mainly of cattail and cattail mix with higher leaf chlorophyll content and lower carotenoids, which are expected to show the opposite effect.

There are several reasons that may explain the difference in the results from both sensors. First, the sampling events were conducted in May 2003, closer to the time of the Landsat ETM+ acquisition, indicating a better approximation of the sensor temporal resolution to the dates of the sampling event. Second, the Landsat ETM+ image was from the end of spring season (February) and this may provide a better representation of seasonal taxonomic variations in periphyton spatial distribution and location in water/soil. Third, during the spring season periphyton tends to be submerged while during the wet season (September) periphyton covers a good portion of the study

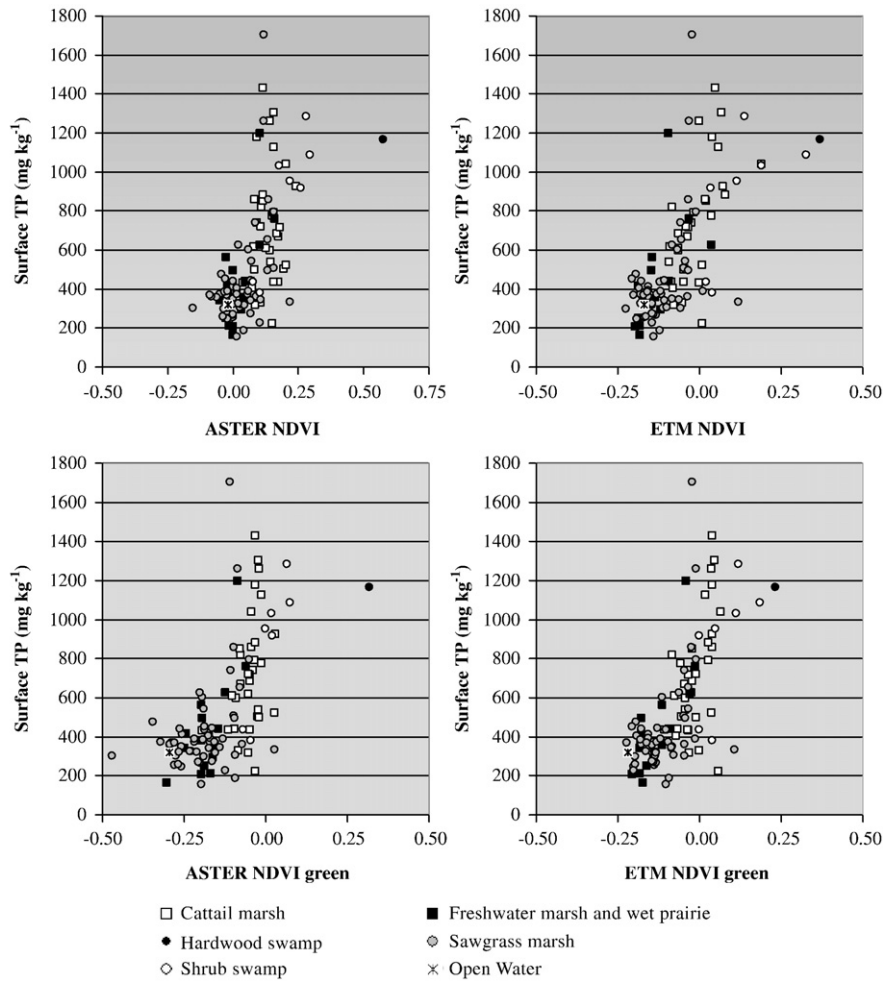


Fig. 6. Scatter plots of surface soil TP against ASTER and Landsat ETM+ values for NDVI and NDVI green with symbols indicating FWC vegetation/land cover class extracted for each sampling point in WCA-2A.

area with floating mats (Figs. 1b and 2). Therefore, differences between Landsat ETM+ and ASTER images may be also indicative of seasonal variations in periphyton, between the summer season and the spring seasons, as documented by McCormick et al. (1996).

NDVI green proved to be the best remote sensing index to predict floc TP in WCA-2A for various reasons. First, there are spatial and seasonal effects of nutrient enrichment associated with various characteristics of periphyton, including biomass, taxonomic composition and TP storage, which have been documented by McCormick et al. (1998). Spatial changes that have been reported by several authors (McCormick et al., 1998; Gaiser et al., 2005) are those associated with the alteration of the diatom community (one of the periphyton algal communities), the collapse of the calcareous periphyton mat (blue-green algae), and its replacement by a non-mat forming algal community dominated by chlorophytes (green algae). The mix of photosynthetic algal pigments (chlorophylls, carotenoids, and phycobilins) is different for each of these algal communities, and these pigments also play different roles in the system. Chlorophylls are responsible for the production of oxygen, while the primary function of almost all carotenoids is photoprotection (i.e., absorbance of high energy on short wavelengths including ultraviolet (UV) and blue regions of the electromagnetic spectrum). These pigments all have in common a maximum reflectance peak in the green band, and a maximum absorbance peak in the blue and the red bands (Richardson, 1996).

The light absorbance properties of water also play a role in the reflectance spectra. Richardson (1996) demonstrated that the overall

signature of multiple carotenoids, chlorophyll *a*, and phycocyanin differ only in the amount of water overlying the algal community. The top spectrum, that is the one acquired by measuring light reflected from a benthic algal community, when it had been removed from the aquatic system (i.e., no overlying water) is the most pronounced, particularly in the IR (above 700 nm). This is due to reemission of light from chlorophyll *a* and it is the red edge that provides the basis for the NDVI applied widely in terrestrial ecosystems. If only 20 cm of water overlie the algal community (middle spectrum), this red emission is strongly attenuated, and it is almost completely absorbed by 2 m of

Table 5

Summary of correlation coefficients (*r*) and coefficients of determination (*R*²) for log-transformed floc and surface soil TP, and NDVI and NDVI green values for each remote sensor (ASTER and Landsat ETM+) in WCA-2A, Everglades.

	<i>r</i>	<i>R</i> ²
<i>Log floc TP – Landsat ETM+ and ASTER remote sensing indices</i>		
Log floc TP – ETM NDVI green	0.83	0.68
Log floc TP – ETM NDVI	0.77	0.59
Log floc TP – ASTER NDVI	0.75	0.56
Log floc TP – ASTER NDVI green	0.72	0.51
<i>Log surface TP – Landsat ETM+ and ASTER remote sensing indices</i>		
Log surf. TP – ETM NDVI green	0.67	0.45
Log surf. TP – ETM NDVI	0.68	0.46
Log surf. TP – ASTER NDVI	0.63	0.39
Log surf. TP – ASTER NDVI green	0.62	0.38

Table 6
Regression model parameters for prediction of log-transformed floc total phosphorus (TP) in mg kg^{-1} in WCA-2A, Everglades.

Model	<i>r</i>	<i>R</i> ²	Adjusted <i>R</i> ²	Std. error of estimate	Regression equation	Significance
Linear ^a	0.83	0.68	0.67	0.119	1.842 + 1.952 (Landsat ETM+ NDVI green)	0.00
Quadratic ^a	0.84	0.71	0.70	0.114	0.713 + 6.236 (Landsat ETM+ NDVI green) – 3.954 (Landsat ETM+ NDVI green) ²	0.00
Multiple ^b	0.87	0.75	0.75	0.105	4.237 + 1.277 (Landsat ETM + NDVIgreen) – 0.0000267 (Distance to Water Control Structures) – 0.00000706 (Y coordinate)	0.01

^a Predictor: Landsat ETM+ NDVI green.

^b Predictors: Landsat ETM+ NDVI green, Distance to Water Control Structures, and Y coordinate (Albers Equal Area Conic map projection).

Table 7
Regression model parameters for prediction of log-transformed soil surface total phosphorus (TP) in mg kg^{-1} in WCA-2A, Everglades.

Model	<i>r</i>	<i>R</i> ²	Adjusted <i>R</i> ²	Std. error of estimate	Regression equation	Significance
Linear Landsat ^a	0.68	0.46	0.46	0.167	1.905 + 1.457 (Landsat ETM+ NDVI)	0.00
Linear Aster ^b	0.63	0.39	0.39	0.177	2.572 + 1.440 (ASTER NDVI)	0.00
Quadratic Landsat ^a	0.71	0.50	0.48	0.162	2.816 + 1.486 (Landsat ETM+ NDVI) – 2.203 (Landsat ETM+ _NDVI)	0.00
Multiple ^c	0.72	0.51	0.50	0.167	2.852 + 1.064 (Landsat ETM+ NDVI) – 0.000015 (distance to water control structures)	0.00

^a Predictor: Landsat ETM+ NDVI.

^b Predictor: ASTER NDVI.

^c Predictors: Landsat ETM+ NDVI, and Distance to Water Control Structure.

overlying water (bottom spectrum). However, the overall signatures, which include the green reflectance peak near 550 nm and the phycocyanin absorption feature at 620 nm, are still discernible under 2 m of water (Richardson, 1996).

7. Conclusions

We conclude that the results obtained with the Landsat ETM+ NDVI green and its capability to capture the spatial variability of floc TP, are associated with variations in periphyton depth (metaphyton, floating mats, and benthic/epipelon periphyton). Variable water depth is captured by the water penetration capabilities of the green band, while the red band is absorbed.

The data derived from ASTER and Landsat ETM+ satellite imagery as secondary variables provided exhaustive coverage to delineate vegetation and periphyton properties that were correlated with floc and soil TP. ASTER data has a higher spatial resolution (15 m) in comparison with Landsat ETM+ (30 m). The spatial resolution of ASTER represents an improvement to represent small features of this landscape such as tree islands, and account for differences in the ridge/slough areas. But in this study the higher spatial resolution image (15 m) did not improve the strength of relationships between spectral and floc and soil TP. This may be explained by the smoothing effect of the coarser image that provided an aggregated response within each 30 m pixels.

The relationships between spectral indices and floc as well as soil TP were stronger when compared to spectral data from different sensors. Spectral data showed stronger relationships when compared to ancillary environmental data such as distance to control structure or tree islands. These results support the hypothesis that spectral data provide an inference mechanism on below-ground properties such as soil TP. This suggests that exhaustive spectral datasets can be incorporated into geostatistical/hybrid models to improve the prediction of site-specific floc and/or soil TP.

We conclude that remote sensing, and particularly NDVI green and NDVI, can be used as indirect indicators to infer on soil nutrient status in this particular wetland area. These methods need to be further tested in other wetland areas across the Everglades or in other similar tropical and subtropical wetlands. If the same relationships found in this study can be replicated in similar landscape settings more generic remote sensing applications that pertain to wetlands could be developed.

Remote sensing images allow repeated monitoring covering large wetland areas that are more cost-effective than labor-intensive and costly soil sampling and laboratory analyses. Even if predictive capabilities based on spectral data are limited they improve our understanding of difficult to observe, buried features (e.g., floc and soil TP). To monitor the soil nutrient status in WCA-2A and other subtropical wetlands that are impacted by nutrient influx is important to assess long-term impacts, their resilience and functions, and recovery or degradation of the ecosystem. Functional relationship between chlorophyll content in the aquatic and vegetated portions of this wetland with soil nutrients should be explored with more detail across nutrient gradients. Spectral techniques and inferential modeling are non-invasive and cost-effective methods to monitor soil nutrient status in complex wetland systems. Remote sensing-based measures have potential to support ongoing restoration efforts in the Everglades outlined in the Comprehensive Everglades Restoration Plan. In addition, spectral inferential modeling has a potential to be applied not only to other wetland areas in the Everglades but also to other biogeochemical properties.

To explicitly incorporate seasonal variability in TP prediction models would allow accounting for phenological and taxonomic variations in vegetation, periphyton, and other components of the system. Although

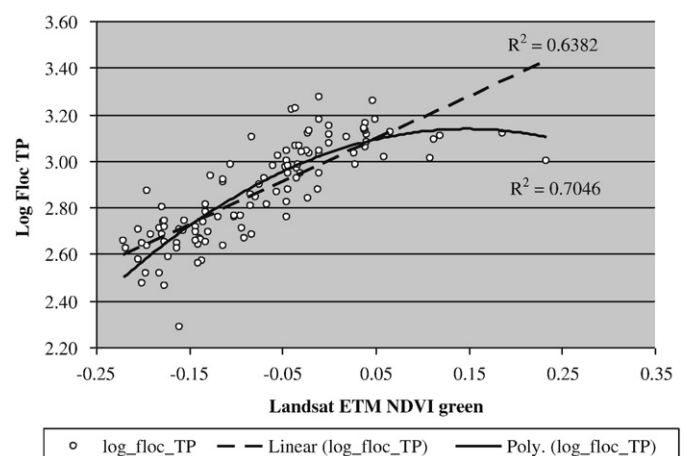


Fig. 7. Comparison between linear and quadratic regression model to predict floc TP with Landsat ETM+ NDVI green in WCA-2A.

cost and accessibility limits the possibility of conducting field sampling during certain times of the year, comparisons with the same sensor during different seasons could address some of the limitations of this research, as well as comparison between sensors during the same sampling event. Multi-temporal pattern analysis of images could provide sequences of biophysical ecosystem responses. However, such analysis would need to be complimented by soil monitoring which is costly and labor-intensive in wetlands such as WCA-2A.

Acknowledgements

This research was partially supported with funds from the South Florida Water Management District and other sources. The authors thank Dr. Sue Newman, South Florida Water Management District, and Dr. K. R. Reddy, Wetland Biogeochemistry Laboratory, Soil and Water Science Department, University of Florida, for allowing us to use their spatial soil phosphorus data in this study.

References

- Ackleson, S. G., & Klemas, V. (1987). Remote sensing of submerged aquatic vegetation in lower Chesapeake Bay: A comparison of Landsat MSS to TM imagery. *Remote Sensing of Environment*, 22, 235–248.
- Anderson, J. M. (1976). An ignition method for determination of total phosphorus in lake sediments. *Water Resources*, 10, 329–331.
- Arst, H. (2003). *Optical properties and remote sensing of multicomponental water bodies*. Chichester, UK: Springer-Praxis.
- Asner, G. P., Wessman, C. A., Schimel, D. S., & Archer, S. (1998). Variability in leaf and litter optical properties: Implications for BRDF model inversions using AVHRR, MODIS, and MISR. *Remote Sensing of Environment*, 63, 243–257.
- Baban, S. M. J. (1997). Environmental monitoring of estuaries; estimating and mapping various environmental indicators in Breydon Water Estuary, U.K., using Landsat TM imagery. *Estuarine Coastal and Shelf Science*, 44, 589–598.
- Boelman, N. T., Stieglitz, M., Rueth, H. M., Sommerkorn, M., Griffin, K. L., Shaver, G. R., & Gamon, J. A. (2003). Response of NDVI, biomass, and ecosystem gas exchange to long-term warming and fertilization in wet sedge tundra. *Oecologia*, 135, 414–421.
- Carter, G. A., Cibula, W. G., & Miller, R. L. (1996). Narrow-band reflectance imagery compared with thermal imagery for early detection of plant stress. *Journal of Plant Physiology*, 148, 515–522.
- Craft, C. B., & Richardson, C. J. (1998). Recent and long-term organic soil accretion and nutrient accumulation in the Everglades. *Soil Science Society of America Journal*, 62, 834–843.
- Craighead, F. C. (1971). *The trees of South Florida: The natural environments and their succession*. Coral Gables, FL: Univ. Miami Press.
- Curran, P. J. (1989). Remote sensing of foliar chemistry. *Remote Sensing of Environment*, 29, 271–278.
- Daughtry, C. S., Walthall, C. L., Kim, M. S., Brown de Colstoun, E., & McMurtrey, J. E., III (2000). Estimating corn leaf chlorophyll concentration from leaf and canopy reflectance. *Remote Sensing of Environment*, 74, 229–239.
- Davis, S. M. (1991). Growth, decomposition, and nutrient retention in *Cladium jamaicense* Crantz and *Typha domingensis* Pers. in the Florida Everglades. *Aquatic Botany*, 40, 203–224.
- Davis, S. (1994). Phosphorus inputs and vegetation sensitivity in the Everglades. In S. M. Davis, & J. C. Odgen (Eds.), *Everglades: The Ecosystem and its Restoration* (pp. 357–378). Delray Beach: St. Lucie Press.
- DeBusk, W. F., Newman, S., & Reddy, K. R. (2001). Spatio-temporal patterns of soil phosphorus enrichment in Everglades Water Conservation Area 2A. *Journal of Environmental Quality*, 30, 1438–1446.
- Filela, I., & Peñuelas, J. (1994). The red edge position and shape as indicators of plant chlorophyll content, biomass and hydric status. *International Journal of Remote Sensing*, 15, 1459–1470.
- Gaiser, E. E., Trexler, J. C., Richards, J. H., Childers, D. L., Lee, D., Edwards, A. L., Scinto, L. J., Jayachandran, K., Noe, G. B., & Jones, R. D. (2005). Cascading ecological effects of low-level phosphorus enrichment in the Florida Everglades. *Journal of Environmental Quality*, 34, 717–723.
- Gao, B. C. (1996). NDWI – A normalized difference water index for remote sensing of vegetation liquid water from space. *Remote Sensing of Environment*, 58, 257–266.
- Gitelson, A. A., & Merzlyak, M. N. (1997). Remote estimation of chlorophyll content in higher plant leaves. *International Journal of Remote Sensing*, 18, 2691–2697.
- Gitelson, A., & Merzlyak, M. N. (1997). Remote estimation of chlorophyll content in higher plant leaves. *International Journal of Remote Sensing*, 18, 291–298.
- Gitelson, A., Kaufman, Y. J., & Merzlyak, M. N. (1996). Use of a green channel in remote sensing of global vegetation from EOD-MODIS. *Remote Sensing of Environment*, 58, 289–298.
- Gleason, P. J., Cohen, A. D., Smith, W. G., Brooks, H. K., Stone, P. A., Goodrich, R. L., & Spackman, W. (1974). The environmental significance of Holocene sediments from the Everglades and saline tidal plain. In P. J. Gleason (Ed.), *Environments of South Florida: present and past. Memoir 2 of the Miami Geological Society* (pp. 297–351). Miami: Miami Geological Society.
- Gleiser, R. M., Gorla, D. E., & Ludueña Almeida, F. F. (1997). Monitoring the abundance of *Aedes (Ochlerotatus) albifasciatus* (Macquart 1838) (Diptera: Culicidae) to the south of Mar Chiquita Lake, central Argentina, with the aid of remote sensing. *Annals of Tropical Medicine and Parasitology*, 91, 917–926.
- Griffith, J. A. (2002). Geographic techniques and recent applications of remote sensing to landscape-water quality studies. *Water, Air and Soil Pollution*, 138, 181–197.
- Grunwald, S. (2006). What do we really know about the space-time continuum of soil-landscapes. In S. Grunwald (Ed.), *Environmental Soil-Landscape Modeling: Geographic Information Technologies and Pedometrics* (pp. 3–36). Boca Raton: CRC Press.
- Grunwald, S., Reddy, K. R., Prenger, J. P., & Fisher, M. M. (2007). Modeling of the spatial variability of biogeochemical soil properties in a freshwater ecosystem. *Ecological Modeling*, 210, 521–535.
- Grunwald, S., Rivero, R. G., & Reddy, K. R. (2007). Understanding spatial variability and its application to biogeochemistry analysis. In D. Sarker, R. Datta, & R. Hannigan (Eds.), *Environmental biogeochemistry – Concepts and case studies* (pp. 435–462). Amsterdam: Elsevier.
- Grunwald, S., Reddy, K. R., Newman, S., & DeBusk, W. F. (2004). Spatial variability, distribution and uncertainty assessment of soil phosphorus in a south Florida wetland. *Environmetrics*, 15, 811–825.
- Grunwald, S., Corstanje, R., Weinrich, B. E., & Reddy, K. R. (2005). Spatial patterns of labile forms of phosphorus in a subtropical wetland. *Journal of Environmental Quality*, 35, 378–389.
- Haack, B. (1996). Environmental auditing: monitoring wetland changes with remote sensing: an east African example. *Environmental Management*, 20, 411–419.
- Harvey, K. R., & Hill, G. J. E. (2001). Vegetation mapping of a tropical freshwater swamp in the Northern Territory, Australia: A comparison of aerial photography, Landsat TM and SPOT satellite imagery. *International Journal of Remote Sensing*, 22, 2911–2925.
- Horler, D. N. H., Dockray, M., & Barber, J. (1983). The red edge of plant leaf reflectance. *International Journal of Remote Sensing*, 4, 273–288.
- Jensen, J. R., Koch, K., Rutchey, M. S., & Narumalani, S. (1995). Inland wetland change detection in the Everglades Water Conservation Area 2A using a time series of normalized remotely sensed data. *Photogrammetric Engineering & Remote Sensing*, 61, 199–209.
- Johnston, R. M., & Barson, M. M. (1993). Remote sensing of Australian wetlands: An evaluation of Landsat TM data for inventory and classification. *Australian Journal of Marine and Freshwater Research*, 44, 235–252.
- Junka, W. J., & Nunes de Cunhab, C. (2005). Pantanal: A large South American wetland at a crossroads. *Ecological Engineering*, 24, 391–401.
- Kelly, J., & Harwell, M. (1990). Indicators of ecosystem recovery. *Environmental Management*, 14, 527–545.
- Koch, M. S., & Reddy, K. R. (1992). Distribution of soil and plan nutrients along a trophic gradient in the Florida Everglades. *Soil Science Society of America Journal*, 56, 1492–1499.
- Lo, C. P., & Watson, L. J. (1998). The influence of geographic sampling methods on vegetation map accuracy evaluation in a swampy environment. *Photogrammetric Engineering & Remote Sensing*, 64, 1189–1200.
- Martin, M. E., & Aber, J. D. (1997). High spectral resolution remote sensing of forest canopy lignin, nitrogen, and ecosystem processes. *Ecological Applications*, 7, 431–443.
- McCormick, P. V., & O'Dell, M. B. (1996). Quantifying periphyton responses to phosphorus enrichment in the Florida Everglades: A synoptic-experimental approach. *Journal of North America Benthology Society*, 15, 450–468.
- McCormick, P. V., & Stevenson, R. J. (1998). Periphyton as a tool for ecological assessment and management in the Florida Everglades. *Journal of Phycology*, 34, 726–733.
- McCormick, P. V., Rawlik, P. S., Lurding, K., Smith, E. P., & Sklar, F. H. (1996). Periphyton-water quality relationships along a nutrient gradient in the northern Florida Everglades. *Journal of North America Benthology Society*, 15, 433–449.
- McCormick, P. V., Shuford, R. B. E., III, Backus, J. G., & Kennedy, W. C. (1998). Spatial and seasonal patterns of periphyton biomass and productivity in the northern Everglades, Florida, U.S.A. *Hydrobiologia*, 362, 185–208.
- McCormick, P. V., Newman, S., Miao, S. L., Reddy, K. R., Rawlik, D., Fitz, H. C., Fontaine, T. D., & Marley, D. (1999). *Ecological needs of the Everglades*. West Palm Beach, FL: South Florida Water Management District.
- McCormick, P. V., Newman, S., Miao, S., Gawiik, D., Marley, D., Reddy, R. K., & Fontaine, T. D. (2001). Effects of anthropogenic phosphorus inputs on the Everglades. In J. W. Porter, & K. G. Porter (Eds.), *The Everglades, Florida Bay, and Coral Reefs of the Florida Keys: An ecosystem sourcebook* (pp. 83–126). Boca Raton: CRC Press.
- Mertes, L., Smith, M., & Adams, J. (1993). Estimating suspended sediment concentrations in surface waters of the Amazon River wetlands from Landsat images. *Remote Sensing of Environment*, 43, 281–301.
- Munn, R. (1988). The design of integrated monitoring systems to provide early indications of environmental/ecological changes. *Environmental Monitoring and Assessment*, 11, 203–217.
- Munyati, C. (2000). Wetland change detection on the Kafue Flats, Zambia, by classification of a multitemporal remote sensing image dataset. *International Journal of Remote Sensing*, 21, 1787–1806.
- Newman, S., Grace, J. B., & Koebel, J. W. (1996). The effects of nutrients and hydroperiod on mixtures of *Typha domingensis*, *Cladium jamaicense*, and *Eleocharis interstincta*: Implications for Everglades restoration. *Ecological Applications*, 6, 774–783.
- Newman, S., Schuette, J., Grace, J. B., Rutchey, K., Fontaine, T., Reddy, K. R., & Pietrucha, M. (1998). Factors influencing cattail abundance in the northern Everglades. *Aquatic Botany*, 60, 265–280.
- Newman, S., McCormick, P. V., Miao, S. L., Laing, J. A., Kennedy, W. C., & O'Dell, M. B. (2004). The effect of phosphorus enrichment on the nutrient status of a northern Everglades slough. *Wetlands Ecology and Management*, 12, 63–79.
- Noe, G. B., Childers, D. L., & Jones, R. D. (2001). Phosphorus biogeochemistry and the impact of phosphorus enrichment: Why is the Everglades so unique? *Ecosystems*, 4, 603–624.

- Numata, I., Soares, J. V., Leonidas, D. A., Roberts, F. C., Chadwick, O. A., & Batista, G. T. (2003). Relationships among soil fertility dynamics and remotely sensed measures across pasture chronosequences in Rondônia, Brazil. *Remote Sensing of Environment*, 87, 446–455.
- Orem, W. H., Willard, D. A., Lerch, H. E., Bates, A. L., Boylan, A., & Comm, M. (2002). Nutrient geochemistry of sediments from two tree islands in Water Conservation Area 3B, the Everglades, Florida. In F. H. Sklar, & A. van der Valk (Eds.), *Tree Islands of the everglades* (pp. 153–186). Boston: Kluwer Academic Publishers.
- Ozesmi, S. L., & Bauer, M. (2002). Satellite remote sensing of wetlands. *Wetland Ecology and Management*, 10, 381–402.
- Peñuelas, J., Filella, I., Biel, C., Serrano, L., & Save, R. (1993). The reflectance at the 950–970 nm region as an indicator of plant water status. *International Journal of Remote Sensing*, 14(10), 1887–1905.
- Peñuelas, J., Piñol, J., Ogaya, R., & Filella, I. (1997). Estimation of plant water concentration by the reflectance water index WI (R900/R970). *International Journal of Remote Sensing*, 18, 2869–2875.
- Pope, K. O., Sheffner, E. J., Linthicum, K. J., Bailey, C. L., Logan, T. M., Kasischke, E. S., Birney, K., Njogu, A. R., & Roberts, C. R. (1992). Identification of central Kenyan Rift Valley Fever virus vector habitats with Landsat TM and evaluation of their flooding status with airborne imaging radar. *Remote Sensing of Environment*, 40, 185–196.
- Qualls, R. G., & Richardson, C. J. (2000). Phosphorus enrichment affects litter decomposition, immobilization, and soil microbial phosphorus in wetland mesocosms. *Soil Science Society of America Journal*, 64, 799–808.
- Quental, N. (2001). *A spectral study of nutrient and disease stress in barley and wheat leaves*. Leuven, Belgic: Katholieke Universiteit.
- Reddy, K. R., Wang, Y., DeBusk, W. F., Fisher, M. M., & Newman, S. (1998). Forms of soil phosphorus in selected hydrologic units of the Florida Everglades. *Soil Science Society of America journal*, 62, 1134–1147.
- Richardson, L. (1996). Remote sensing of algal bloom dynamics. *BioScience*, 46, 492–501.
- Rivero, R. G., Grunwald, S., & Bruland, G. L. (2007). Incorporation of spectral data into multivariate geostatistical models to map soil phosphorus variability in a Florida wetland. *Geoderma*, 140, 428–443.
- Rivero, R. G., Grunwald, S., Osborne, T. Z., Reddy, K. R., & Newman, S. (2007). Characterization of the spatial distribution of soil properties in Water Conservation Area 2A, Everglades, Florida. *Soil Science*, 172, 149–166.
- Rouse, J. W., Jr., Haas, R. H., Schell, J. A., & Deering, D. W. (1973). Monitoring vegetation systems in the Great Plains with ERTS. *Third ERTS Symposium, NASA SP-351 I* (pp. 309–317).
- Rutchey, K., & Vilchek, L. (1994). Development of an Everglades vegetation map using a SPOT image and the Global Positioning System. *Photogrammetric Engineering & Remote Sensing*, 60, 767–775.
- Rutchey, K., & Vilchek, L. (1999). Air photointerpretation and satellite imagery analysis techniques for mapping cattail coverage in a Northern Everglades impoundment. *Photogrammetric Engineering & Remote Sensing*, 65, 185–191.
- Sader, S. A., Ahl, D., & Liou, W. S. (1995). Accuracy of Landsat-TM and GIS rule-based methods for forest wetland classification in Maine. *Remote Sensing of Environment*, 53, 133–144.
- Sahagian, D., & Melack, J. (1996). Global wetland distribution and functional characterization: trace gasses and the hydrological cycle. *Report from the joint GAIM-DIS-BAHC-IGAC-LUCC workshop*. Santa Barbara, CA.
- Scinto, L. J., & Reddy, K. R. (2003). Biotic and abiotic uptake of phosphorus by periphyton in a subtropical freshwater wetland. *Aquatic Botany*, 77, 203–222.
- Townsend, P. A., & Walsh, S. J. (2001). Remote sensing of forested wetlands: Application of multitemporal and multispectral satellite imagery to determine plant community composition and structure in southeastern USA. *Plant Ecology*, 157, 129–149.
- Tucker, C. J. (1979). Red and photographic infrared linear combinations for monitoring vegetation. *Remote Sensing of Environment*, 8, 127–150.
- U.S. Environmental Protection Agency (1993). *Methods for the determination of inorganic substances in environmental samples*. Cincinnati, OH: Environmental Monitoring Systems Lab.
- Ustin, S. L., Roberts, D. A., Gamon, J. A., Asner, G. P., & Green, R. O. (2004). Using imaging spectroscopy to study ecosystem processes and properties. *Bioscience*, 54, 523–534.
- Wu, Y., Sklar, F. H., & Rutchey, K. (1997). Analysis and simulations of fragmentation patterns in the Everglades. *Ecological Applications*, 7, 268–276.